![PeerJ] **Chemistry Journals**
Analytical, Inorganic, Organic, Physical, Materials Science

Characterization and function of medium and large extracellular vesicles from plasma and urine by surface antigens and Annexin V

Ko Igami [1, 2, 3] , Takeshi Uchiumi [Corresp., 1, 4] , Saori Ueda [1] , Kazuyuki Kamioka [2, 5] , Daiki Setoyama [1] , Kazuhito Gotoh [1] , Masaru Akimoto [1] , Shinya Matsumoto [1] , Dongchon Kang [1]

1 Department of Clinical Chemistry and Laboratory Medicine, Kyushu University Graduate School of Medical Sciences, Kyushu University, Fukuoka, Japan

2 Kyushu Pro Search Limited Liability Partnership, Fukuoka, Japan

3 Business Management Division, Clinical Laboratory Business Segment, LSI Medience Corporation, Tokyo, Japan

4 Clinical Chemistry, Division of Biochemical Science and Technology, Department of Health Sciences, Faculty of Medical Sciences,, Kyushu University, Fukuoka, Japan

5 Department of Medical Solutions, LSI Medience Corporation, Tokyo, Japan

Corresponding Author: Takeshi Uchiumi
Email address: uchiumi@cclm.med.kyushu-u.ac.jp

Background. Extracellular vesicles (EVs) are released by most cell types and are involved in multiple basic biological processes. Medium/large EVs (m/lEVs), which is different size from exosome, plays an important role in the coagulation in blood, and is secreted from cancer cells, etc., suggesting functions related to malignant transformation. The m/lEVs levels in blood or urine may help unravel pathophysiological findings in many diseases. However, it remains unclear how many naturally-occurring m/lEV subtypes exist as well as how their characteristics and functions differ from one another. **Methods**. We used the blood and urinal sample from each 10 healthy donors for analysis. Using a flow cytometer, we focus on characterization of EVs with large sizes (>200nm) that are different from exosomes. We also searched for a membrane protein for characterization with a flow cytometer using shotgun proteomics. Then we identified m/lEVs pelleted from plasma and urine samples by differential centrifugation and characterized by flow cytometry. **Results**. Using proteomic profiling, we identified several proteins involved in m/lEV biogenesis including adhesion molecules, peptidases and exocytosis regulatory proteins. In healthy human plasma, we could distinguish m/lEVs derived from platelets, erythrocytes, monocytes/macrophages, T and B cells, and vascular endothelial cells with more than two positive surface antigens. The ratio of phosphatidylserine appearing on the membrane surface differed depending on the cell-derived m/lEVs. In urine, 50% of m/lEVs were Annexin V negative but contained various membrane peptidases derived from renal tubular villi. Urinary m/lEVs, but not plasma m/lEVs, showed peptidase activity. The knowledge of the new characteristics is considered to be useful as a diagnostic material

and the newly developed method suggests the possibility of clinical application.

1 Characterization and function of medium and large extracellular vesicles from plasma and urine

2 by surface antigens and Annexin V

4 Ko Igami[1, 2, 3], Takeshi Uchiumi[1,4]*, Saori Ueda[1], Kazuyuki Kamioka[2, 5], Daiki Setoyama[1],

5 Kazuhito Gotoh[1], Masaru Akimoto[1], Shinya Matsumoto[1] and Dongchon Kang[1]

7 [1]Department of Clinical Chemistry and Laboratory Medicine, Kyushu University Graduate

8 School of Medical Sciences, 3-1-1, Maidashi, Higashi-ku, Fukuoka 812-8582, Japan.

9 [2]Kyushu Pro Search Limited Liability Partnership, 4-1, Kyudaishimmachi, Nishi-ku, Fukuoka,

10 819-0388, Japan.

11 [3]Business Management Division, Clinical Laboratory Business Segment, LSI Medience

12 Corporation, 13-4, Uchikanda 1-chome, Chiyoda-ku, Tokyo, 101-8517, Japan.

13 [4]Clinical Chemistry, Division of Biochemical Science and Technology, Department of Health

14 Sciences, Faculty of Medical Sciences, Kyushu University, Fukuoka, Japan

15 [5] Department of Medical Solutions, LSI Medience Corporation, 3-30-1, Shimura, Itabashi-ku,

16 Tokyo, 174-8555, Japan.

18 *Correspondence Author:

19 Takeshi Uchiumi, Department of Clinical Chemistry and Laboratory Medicine, Kyushu

20 University Graduate School of Medical Sciences, 3-1-1, Maidashi, Higashi-ku, Fukuoka 812-

21 8582, Japan.

22 E-mail: uchiumi@cclm.med.kyushu-u.ac.jp

24 **Abstract**

25 **Background**. Extracellular vesicles (EVs) are released by most cell types and are involved in

26 multiple basic biological processes. Medium/large EVs (m/lEVs), which is different size from

27 exosome, plays an important role in the coagulation in blood, and is secreted from cancer cells,

28 etc., suggesting functions related to malignant transformation. The m/lEVs levels in blood or

29 urine may help unravel pathophysiological findings in many diseases. However, it remains

30 unclear how many naturally-occurring m/lEV subtypes exist as well as how their characteristics

31 and functions differ from one another.

32 **Methods**. We used the blood and urinal sample from each 10 healthy donors for analysis. Using

33 a flow cytometer, we focus on characterization of EVs with large sizes (>200nm) that are

34 different from exosomes. We also searched for a membrane protein for characterization with a

35 flow cytometer using shotgun proteomics. Then we identified m/lEVs pelleted from plasma and

36 urine samples by differential centrifugation and characterized by flow cytometry.

37 **Results**. Using proteomic profiling, we identified several proteins involved in m/lEV biogenesis

38 including adhesion molecules, peptidases and exocytosis regulatory proteins. In healthy human

39 plasma, we could distinguish m/lEVs derived from platelets, erythrocytes,

40 monocytes/macrophages, T and B cells, and vascular endothelial cells with more than two

41 positive surface antigens. The ratio of phosphatidylserine appearing on the membrane surface

42 differed depending on the cell-derived m/lEVs. In urine, 50% of m/lEVs were Annexin V

43 negative but contained various membrane peptidases derived from renal tubular villi. Urinary

44 m/lEVs, but not plasma m/lEVs, showed peptidase activity. The knowledge of the new

45 characteristics is considered to be useful as a diagnostic material and the newly developed

46 method suggests the possibility of clinical application.

47

48 **Introduction**

49   Extracellular vesicles (EVs) play essential roles in cell-cell communication and are

50 diagnostically significant molecules. EVs are secreted from most cell types under normal and

51 pathophysiological conditions (Iraci et al. 2016; Ohno et al. 2013). These membrane vesicles can

52 be detected in many human body fluids and are thought to have signaling functions in

53 interactions between cells. Analysis of EVs may have applications in therapy, prognosis, and

54 biomarker development in various fields. The hope is that using EV analysis, clinicians will be

55 able to detect the presence of disease as well as to classify its progression using noninvasive

56 methods such as liquid biopsy (Boukouris & Mathivanan 2015; Piccin 2014; Piccin et al. 2015a;

57 Piccin et al. 2017a; Piccin et al. 2017b; Piccin et al. 2015b).

58   Medium/large extracellular vesicles (m/lEVs) can be classified based on their cellular

59 origins, biological functions and biogenesis (El Andaloussi et al. 2013). In a broad sense, they

60 can be classified into m/lEVs with diameters of 100–1000 nm diameter (membrane blebs) and

61 smaller EVs (e.g. exosomes) with diameters of 30–150 nm (Raposo & Stoorvogel 2013; Robbins

62 & Morelli 2014). The m/lEVs are generated by direct outward budding from the plasma

63 membrane (D'Souza-Schorey & Clancy 2012), while smaller EVs (e.g. exosomes) are produced

64 via the endosomal pathway with formation of intraluminal vesicles by inward budding of

65 multivesicular bodies (MVBs) (Raposo & Stoorvogel 2013). In this study, we analyzed the

66 physical characteristics of EVs from 200 nm to 800 nm in diameter which we refer to as m/lEVs

67 as per the MISEV2018 guidelines (Thery et al. 2018).

68   Recently, the clinical relevance of EVs has attracted significant attention. In particular,

69 m/lEVs play an important role in tumor invasion (Clancy et al. 2015).   m/lEVs in blood act as a

70 coagulant factor and have been associated with sickle cell disease, sepsis, thrombotic

71 thrombocytopenic purpura, and other diseases (Piccin et al. 2007; Piccin et al. 2017a; Piccin et

72 al. 2017b). A possible role for urinary m/lEVs in diabetic nephropathy was also reported (Sun et

73 al. 2012). In recent years, the clinical applications of exosomes have been developed (Yoshioka

74 et al. 2014). However, because characterization of exosomes is analytically challenging,

75 determining the cells and tissues from which exosomes are derived can be difficult. m/lEVs are

76   generated differently from exosomes (Mathivanan et al. 2010) but are similar in size and contain

77   many of the same surface antigens. It is widely hypothesized that complete separation of

78   exosomes and m/lEVs is likely to be a major challenge, and more effective techniques to purify

79   and characterize m/lEVs would be extremely valuable.

80   In this study, we focused on m/lEVs in plasma and urine, which are representative body fluids in

81   clinical laboratories. We purified for m/lEVs based on differential centrifugation and

82   characterized m/lEVs by flow cytometry and mass spectrometry analysis and described the basic

83   properties (characterizing surface antigen and orientation of phosphatidylserine and activity of

84   the enzymes) of m/lEV subpopulations in blood and urine.

85

86

87 **Materials and Methods**

88 **Antibodies and other reagents**

89 The following monoclonal antibodies against human surface antigens were used in this study:

90 anti-CD5(clone: L17F12), anti-CD15 (clone: W6D3), anti-CD41(clone: HIP8), anti-CD45(clone:

91 HI30), anti-CD59 (clone: p282), anti-CD61 (clone: VI-PL2), anti-CD105 (clone: 43A3), anti-

92 CD146(clone: P1H12), anti-CD235a (clone: HI264), anti-CD10 (clone: HI10a), anti-CD13

93 (clone: WM15), anti-CD26 (clone: BA5b), anti-CD227 (MUC1) (clone: 16A). All antibodies

94 were purchased from BioLegend® (San Diego, CA). FITC-conjugated Annexin V was

95 purchased from BD Biosciences (New Jersey, USA). We used the SPHERO™ Nano Fluorescent

96 Particle Size Standard Kit, Yellow (diameters 0.22, 0.45, 0.88 and 1.35 μm) from Spherotech

97 Inc. for size validation. Normal mouse IgG was purchased from Wako Chemicals (Tokyo,

98 Japan). APC-conjugated normal mouse IgG was produced using the Mix-n-Stain™ APC

99 Antibody Labeling kit from Biotium Inc. Dithiothreitol (DTT) was purchased from Wako

100 Chemicals (Tokyo, Japan). We conducted phase transfer surfactant experiments using "MPEX

101 PTS Reagents for MS" purchased from GL Sciences Inc. and "Trypsin, TPCK Treated"

102 purchased from Thermo Fisher Scientific™. Iodoacetamide was purchased from Wako

103 Chemicals (Tokyo, Japan).

104 **Samples**

105 All studies were approved by the Institutional Review Board of the Kyushu University Hospital,

106 Kyushu University (29-340). Blood samples were collected from 20 male and female

107 participants (23–48 years of age) who were apparently healthy. We received the informed

108 consent from all participants of this study. Samples were collected using a 22-gauge butterfly

109 needle and a slow-fill syringe. After discarding the initial 2–3 mL, blood was dispensed into

110 collection tubes containing ethylenediamine tetra acetic acid (EDTA) (1.6 mg/mL blood). Urine

111 was collected from 20 male healthy subjects (23–46 years of age). The first morning void urine

112 was used for the experiments. The urine samples were collected in a sterile container. In

113 particular, we confirmed that sample used for analysis by flow cytometer were derived from

114   healthy donors by measuring blood count and creatinine in blood and total urine protein

115   (Supplementary Table.S1).

116   **Isolation of plasma m/lEVs**

117   Essentially platelet-free plasma (PFP) was prepared from EDTA-treated blood by double

118   centrifugation at 2,330 ×g for 10 min. To assess residual platelets remaining in this sample, we

119   measured platelet number using the ADVIA® 2120i Hematology System (SIEMENS

120   Healthineers, Erlangen Germany). The number of platelets in this sample was below the limit of

121   detection (1×10^3 cells/μL). We used a centrifugation method to obtain m/lEVs. In an effort to

122   ensure our approach could be applied to clinical testing, we chose a simple and easy method for

123   pretreatment. In an ISEV position paper (Mateescu et al. 2017), Thery's group referred to

124   vesicles sedimenting at 100,000 ×g as "small EVs" rather than exosomes, those pelleting at

125   intermediate speed (lower than 20,000 ×g) as "medium EVs" (including microvesicles and

126   ectosomes) and those pelleting at low speed (e.g., 2000 ×g) as "large EVs". Because these

127   definitions are less biologically meaningful but more experimentally tractable than previously-

128   applied exosome/microvesicle definitions, we attempted biological characterization through

129   subsequent shotgun and flow cytometry analysis.

130   In flow cytometric analysis, the volume of PFP used in each assay was 0.6 mL from each

131   donor. In electron microscopy, the volume of PFP used was 3 mL. Samples were independent

132   and were treated individually prior to each measurement. PFP was centrifuged at 18,900 ×g for

133   30 min in a fixed-angle rotor. The m/lEV pellet obtained after centrifugation was reconstituted

134   by vortex mixing (1–2 min) with an equivalent volume of Dulbecco's phosphate-buffered saline

135   (DPBS), pH 7.4. The solution was centrifuged at 18,900 ×g for 30 min again and the supernatant

136   was discarded.

137   **Isolation of urinary m/lEVs**

138   For isolation of urinary m/lEVs, we modified a urinary exosome extraction protocol (Fernandez-

139   Llama et al. 2010). The centrifugation conditions were identical for plasma and urine so that the

140   size and the density of m/lEVs were similar, enabling comparison of plasma and urinary m/lEVs.

141   In flow cytometric analysis, the volume of urine used for each assay was 1.2 mL from

142   each donor. In electron microscopy, the volume of urine used was 15 mL. Samples were

143   independent and were treated individually prior to each measurement. Collected urine was

144   centrifuged at 2,330 $\times g$ for 10 min twice. The supernatant was centrifuged at 18,900 $\times g$ for 30

145   min in a fixed-angle rotor. The m/lEV pellet obtained from centrifugation was reconstituted by

146   vortex mixing (1–2 min) with 0.2 mL of DPBS followed by incubation with DTT (final

147   concentration 10 mg/mL) at 37°C for 10–15 min. The samples were centrifuged again at 18,900

148   $\times g$ for 30 min and the supernatant was discarded. Addition of DTT, a reducing agent, reduced

149   the formation of Tamm-Horsfall protein (THP) polymers. THP monomers were removed from

150   m/lEVs after centrifugation. DTT-containing DPBS solutions were filtered through 0.1-µm

151   filters (Millipore).

152   **Flow cytometric analysis of m/lEVs**

153   After resuspending m/lEV pellets in 60 µL of DPBS, we added saturating concentrations of

154   several labelled antibodies, Annexin V and normal mouse IgG and incubated the tubes in the

155   dark, without stirring, for 15–30 min at room temperature. In one case, we added labelled

156   antibodies directly to 60 µL of PFP for staining. We resuspended stained fractions in Annexin V

157   binding buffer (BD Biosciences: 10 mM HEPES, 0.14 mM NaCl, 2.5 mM $CaCl_2$, pH 7.4) for

158   analysis by flow cytometry. DPBS and Annexin V binding buffer were filtered through 0.1-µm

159   filters (Millipore). Flow cytometry was performed using a FACSVerse™ flow cytometer (BD

160   Biosciences). The flow cytometer was equipped with 405 nm, 488 nm and 638 nm lasers to

161   detect up to 13 fluorescent parameters. The flow rate was 12 µL/min. Forward scatter voltage

162   was set to 381, side scatter voltage was set to 340, and each threshold was set to 200. Details of

163   excitation (Ex.) and emission (Em.) wavelengths as well as voltages described in supplements

164   Fig. Flow cytometry was performed using FACSuite™ software (BD Biosciences) and data were

165   analyzed using FlowJo software. The authors have applied for the following patents for the

166   characterization method of m/lEVs isolated from plasma and urine with a flow cytometer:

167   JP2018-109402(plasma) and JP2018-109403(urine).

168   **Nanoparticle tracking analysis (NTA)**

169 NTA measurements were performed using a NanoSight LM10 (NanoSight, Amesbury, United

170 Kingdom). After resuspending mEV pellets in 50 μL of DPBS, samples were diluted eight-fold

171 (plasma) and 100-fold (urinary) with PBS prior to measurement. Particles in the laser beam

172 undergo Brownian motion and videos of these particle movements are recorded. NTA 2.3

173 software then analyses the video and determines the particle concentration and the size

174 distribution of the particles. Twenty-five frames per second were recorded for each sample at

175 appropriate dilutions with a "frames processed" setting of 1500. The detection threshold was set

176 at "7 Multi" and at least 1,000 tracks were analyzed for each video.

177 **Electron microscopy**

178 For immobilization, we added 100 μL of PBS and another 100 μL of immobilization solution

179 (4% paraformaldehyde, 4% glutaraldehyde, 0.1 M phosphate buffer, pH 7.4) to m/lEV pellets.

180 After stirring, we incubated at 4°C for 1 h. For negative staining, the samples were adsorbed to

181 formvar film-coated copper grids (400 mesh) and stained with 2% phosphotungstic acid, pH 7.0,

182 for 30 s. For observation and imaging, the grids were observed using a transmission electron

183 microscope (JEM-1400Plus; JEOL Ltd., Tokyo, Japan) at an acceleration voltage of 100 kV.

184 Digital images (3296 × 2472 pixels) were taken with a CCD camera (EM-14830RUBY2; JEOL

185 Ltd., Tokyo, Japan).

186 **Protein digestion**

187   We used approximately 50 mL of pooled healthy plasma and 100 mL of pooled healthy

188 male urine from five healthy subjects for digestion of m/lEVs.

189   In plasma the following process is the same as "Isolation of plasma m/lEVs" section. We

190 repeated 18,900 ×g centrifugation washing steps three times to reduce levels of contaminating

191 free plasma proteins and small EVs for shotgun analysis. After the last centrifugation, we

192 removed supernatants and froze the samples.

193   In urine the following process is the same as "Isolation of urinary m/lEVs" section. We

194 repeated washing steps twice (after DTT treatment) to reduce levels of contaminating free

195 urinary proteins and small EVs for shotgun analysis. We removed supernatants and froze the

196 samples.

197   To discover characterizing surface antigen by flowcytometry, the sample was digested

198   using a phase transfer surfactant-aided procedure so that many hydrophobic membrane proteins

199   could be detected (Chen et al. 2017). The precipitated frozen fractions of plasma and urine were

200   thawed at 37°C, and then m/lEVs were solubilized in 250 μL of lysis buffer containing 12 mM

201   sodium deoxycholate and 12 mM sodium lauroyl sarcosinate in 100 mM Tris·HCl, pH 8.5. After

202   incubating for 5 min at 95°C, the solution was sonicated using an ultrasonic homogenizer.

203   Protein concentrations of the solutions were measured using a bicinchoninic acid assay (Pierce™

204   BCA Protein Assay Kit; Thermo Fisher Scientific).

205   Twenty microliters of the dissolved pellet (30 μg protein) were used for protein digestion.

206   Proteins were reduced and alkylated with 1 mM DTT and 5.5 mM iodoacetamide at 25°C for 60

207   min. Trypsin was added to a final enzyme:protein ratio of 1:100 (wt/wt) for overnight digestion.

208   Digested peptides were acidified with 0.5% trifluoroacetic acid (final concentration) and 100 μL

209   of ethyl acetate was added for each 100 μL of digested m/lEVs. The mixture was shaken for 2

210   min and then centrifuged at 15,600 $\times g$ for 2 min to obtain aqueous and organic phases. The

211   aqueous phase was collected and desalted using a GL-Tip SDB column (GL Sciences Inc).

212   **LC-MS/MS analysis**

213   Digested peptides were dissolved in 40 μL of 0.1% formic acid containing 2% (v/v) acetonitrile

214   and 2 μL were injected into an Easy-nLC 1000 system (Thermo Fisher Scientific). Peptides were

215   separated on an Acclaim PepMap™ RSLC column (15 cm × 50 μm inner diameter) containing

216   C18 resin (2 μm, 100 Å; Thermo Fisher Scientific™), and an Acclaim PepMap™ 100 trap

217   column (2 cm× 75 μm inner diameter) containing C18 resin (3 μm, 100 Å; Thermo Fisher

218   Scientific™). The mobile phase consisted of 0.1% formic acid in ultrapure water (buffer A). The

219   elution buffer was 0.1 % formic acid in acetonitrile (buffer B); a linear 200 min gradient from

220   0%–40% buffer B was used at a flow rate of 200 nL/min. The Easy-nLC 1000 was coupled via a

221   nanospray Flex ion source (Thermo Fisher Scientific™) to a Q Exactive™ Orbitrap (Thermo

222   Fisher Scientific™). The mass spectrometer was operated in data-dependent mode, in which a

223   full-scan MS (from 350 to 1,400 m/z with a resolution of 70,000, automatic gain control (AGC)

224   3E+06, maximum injection time 50 ms) was followed by MS/MS on the 20 most intense ions

225 (AGC 1E+05, maximum injection time 100 ms, 4.0 m/z isolation window, fixed first mass 100

226 m/z, normalized collision energy 32 eV).

Proteome Data Analysis

228 Raw MS files were analyzed using Proteome Discoverer software version 1.4 (Thermo Fisher

229 Scientific™) and peptide lists were searched against the Uniprot Proteomes-Homo sapiens

230 FASTA (Last modified November 17, 2018) using the Sequest HT algorithm. Initial precursor

231 mass tolerance was set at 10 ppm and fragment mass tolerance was set at 0.6 Da. Search criteria

232 included static carbamidomethylation of cysteine (+57.0214 Da), dynamic oxidation of

233 methionine (+15.995 Da) and dynamic acetylation (+43.006 Da) of lysine and arginine residues.

Gene ontology analysis and gene enrichment analysis

235 We conducted GO analysis using DAVID (https://david.ncifcrf.gov) to categorize the

236 proteins identified by shotgun analysis and used Metascape

237 (http://metascape.org/gp/index.html#/main/step1) for gene enrichment analysis. We uploaded the

238 UNIPROT_ACCESSION No. for each protein.

Extracellular vesicle preparation from isolated erythrocytes

240 Whole blood was collected by the same method as above and centrifuged at 2,330 $\times g$

241 for 10 min. After removal of the buffy coat and supernatant plasma, the remaining erythrocytes

242 were washed three times by centrifugation at 2,330 $\times g$ for 10 min and the erythrocyte pellet was

243 resuspended in DPBS. EVs were generated from the washed erythrocytes by stimulation in the

244 presence of 2.5 mM $CaCl_2$ (10 mM HEPES, 0.14 mM NaCl, 2.5 mM $CaCl_2$, pH 7.4) for 1 h at

245 room temperature under rotating conditions. Erythrocytes were removed by centrifugation at

246 2,330 $\times g$ for 10 min and the EV rich supernatant was subsequently centrifuged (18,900 $\times g$ for 30

247 min) to pellet the EVs. EVs were resuspended in DPBS.

Dipeptidyl peptidase IV (DPP4:CD26) activity assay

249 DPP4 activity was measured in the plasma and urine of six individuals (different from

250 plasma donors). The method was previously published in part (Kawaguchi et al. 2010). DPP4

251 activity was measured via the fluorescence intensity of 7-amino-4-methylcoumarin (AMC) after

252 its dissociation from the synthetic substrate (Gly-Pro-AMC • HBr) catalyzed by DPP4.

253   Experiments were performed in 96-well black plates. Titrated AMC was added to each well to

254   prepare a standard curve. Fluorescence intensity was measured after incubating substrate with

255   urine samples for 10 min. The enzyme reaction was terminated by addition of acetic acid. The

256   fluorescence intensity (Ex. = 380 nm and Em. = 460 nm) was measured using Varioskan Flash

257   (Thermo Fisher Scientific™). DPP4 activity assays were performed by Kyushu Pro Search LLP

258   (Fukuoka, Japan).

259 **Results**

260 **Isolation and characterization of m/lEVs from plasma and urine.**

261   The workflow for the isolation and enrichment of m/lEVs for flow cytometric analyses is

262 illustrated in Fig.1A and 1B. m/lEVs from human plasma samples were isolated by high-speed

263 centrifugation, an approach used in previous studies (Jayachandran et al. 2012). For isolation of

264 m/lEVs from urine, DTT, a reducing agent, was used to remove THP polymers because these

265 non-specifically interact with IgGs.

266   Transmission electron microscopy revealed that almost all m/lEVs were small, closed

267 vesicles with a size of approximately 200 nm that were surrounded by lipid bilayer (Fig. 1C–H).

268 In plasma, we observed EVs whose membranes were not stained either inside or on the surface

269 (Fig. 1C, 1D); we also observed EVs whose forms were slightly distorted (Fig. 1E). In urine, a

270 group of EVs with uneven morphology and EVs with interior structures were observed (Fig. 1F–

271 1H). Apoptotic bodies, cellular debris, and protein aggregates were not detected.

272   No EVs with diameters greater than 800 nm were observed by NTA (Supplementary

273 Fig.S1) and flow cytometry can detect only EVs with diameters larger than 200 nm. Together,

274 these data suggested that we characterized m/lEVs between 200 nm and 800 nm in diameter

275 from plasma and urine by flow cytometry analysis. We observed the m/lEVs less than 100 nm by

276 NTA because of some contamination or degradation after purification (Supplementary Fig.S1)."

277   Side-scatter events from size calibration beads of (diameters: 0.22, 0.45, 0.88 and 1.35

278 μm) were resolved from instrument noise using a FACS Verse flow cytometer (Supplementary

279 Fig.S2A). Inspection of the side-scatter plot indicated that 0.22 μm was the lower limit for bead

280 detection. More than 90% of m/lEVs isolated from plasma and urine showed side-scatter

281 intensities lower than those of 0.88-μm calibration beads (Fig. 2A–D). m/lEVs were

282 heterogeneous in size, with diameters ranging from 200–800 nm in plasma and urine (Fig. 2A–

283 D). Fluorescently-labeled mouse IgG was used to exclude nonspecific IgG-binding fractions

284 (Supplementary Fig.S2 B and C). In this experiment, we characterized m/lEVs with diameters

285 ranging from 200–800 nm. NTA analysis shows less than 100nm size particles in the plasma

286 fraction extracted by centrifugation, but we focused on particles over 200nm using a flow

287   cytometer. Using these methods, we observed an average of 8×10^5 and 1×10^5 m/lEVs in each mL

288   of plasma and urine by flow cytometry observation.

289   **Shotgun proteomic analysis of plasma and urine EVs.**

290   To analyze the protein components and discover characterizing surface antigen of m/lEVs

291   present in plasma and urine of five healthy individuals, we performed LC-MS/MS proteomic

292   analysis. In this analysis, in order to prevent small EVs contamination, the washing process by

293   centrifugation was increased compared to other analyses (Materials and Methods). A total of 593

294   and 1,793 proteins were identified in m/lEVs from plasma and urine, respectively (Fig. 3A and

295   Supplementary Table S2 and Table S3). Scoring counts using the SequestHT algorithm for the

296   top 20 most abundant proteins are shown in Table 1 and 2. We detected cytoskeleton-related

297   protein such as actin, ficolin-3 and filamin and cell-surface antigen such as CD5, band3 and

298   CD41 in plasma. We also identified actin filament-related proteins such as ezrin, radixin, ankylin

299   and moesin which play key roles in cell surface adhesion, migration and organization   in both

300   plasma and urine. In urine, several types of peptidases (membrane alanine aminopeptidase or

301   CD13; neprilysin or CD10; DPP4 or CD26) and MUC1 (mucin 1 or CD227) were detected in

302   high abundance, and these proteins were used to characterize m/lEVs by flow cytometric

303   analysis (Table 2 and Supplementary Table S3). We demonstrated that the isolated m/lEVs

304   showed high expression of tubulin and actinin, while the tetraspanins CD9 and CD81 that are

305   often used as exosome markers were only weakly identified. Especially in plasma, small EV

306   (exosome) markers TSG101, VPS4 and Alix were not observed in this m/lEVs fraction

307   (Supplementary Table S4). These data suggest that m/lEVs differ from small EVs including

308   exosomes.

309   As shown in Fig. 3A and Supplementary Fig S3, about 10% of urinary EVs proteins were

310   also identified in plasma EVs. Urinary EVs in the presence of blood contaminants were also

311   observed in previous studies (Smalley et al. 2008). These result suggest that m/lEVs in plasma

312   were excreted in the urine via renal filtration and not reabsorbed. Gene ontology analysis of the

313   identified proteins indicated overall similar cellular components in plasma and urine m/lEVs

314   (Fig. 3B). The results of gene set enrichment analysis by metascape are shown for plasma and

315 urine m/lEVs (Fig. 3C, D and Supplementary Table S5 and Table S6). The most commonly-

316 observed functions in both plasma and urine were "regulated exocytosis", "hemostasis" and

317 "vesicle-mediated transport". In plasma, several functions of blood cells were observed,

318 including "complement and coagulation cascades" and "immune response". Moreover, analysis

319 of urinary EVs showed several characteristic functions including "transport of small molecules",

320 "metabolic process" and "cell projection assembly". This may reflect the nature of the kidney,

321 the urinary system and tubular villi. These data demonstrate the power of data-driven biological

322 analyses.

323 **Characterization of plasma EVs by flow cytometry.**

324   Next, we characterized m/lEVs in plasma by flow cytometry using antibodies against

325 several surface antigens and Annexin V. To eliminate nonspecific adsorption, we excluded the

326 mouse IgG-positive fraction. (Supplementary Fig.S2B) Eliminating non-specific reactions to

327 antibodies is important in using human body fluids as diagnostic materials for immunological

328 measurements. By adding mouse IgG-APC to the system, we observed accurate flow cytometry

329 image in which specific surface antigens were recognized by following two points: 1) blocking

330 of non-specific reaction sites, 2) gate-out of positive non-specific reaction. We characterized

331 positive m/lEVs using surface antigens detected by shotgun proteomic analysis and Annexin V

332 (Fig. 4A–L).

333   To characterize m/lEVs derived from erythrocytes, T and B cells,

334 macrophages/monocytes, granulocytes, platelets and endothelial cells, we selected nine antigens

335 described in Fig. 4A. Two or more antigens were used for characterization of m/lEVs: for

336 example, CD59 and CD235a double-positive and CD45-negative m/lEVs were classified as

337 erythrocyte-derived m/lEVs (Supplementary Fig. S4B).   We confirmed that m/lEVs isolated

338 from erythrocytes in vitro and erythrocytes derived m/lEVs from plasma are characterized by

339 CD59 and CD235a double-positive and CD45-negative (Supplementary Fig. S5). Determined

340 positive area by addition of EDTA (Supplementary Fig. S2D), we also show Annexin V staining

341 for the m/lEVs corresponding to these five classifications (Fig. 4B–L). We integrated these

342 characterizations and assessed the distribution of EV classifications among ten healthy subjects

343 (Fig. 4M). The results suggested that no major differences in the ratios of fractions in these ten

344 subjects and thus these definitions may be used for pathological analysis.

345 We found that 10% and 35% of m/lEVs were derived from erythrocytes and platelets,

346 respectively. However, only 0.5%, 0.6% and 0.1% of m/lEVs were derived from macrophages,

347 leukocytes and endothelial cells, respectively suggesting that the ratio of m/lEVs of different

348 cellular origins is dependent on the number of cells present in plasma (Fig. 4M). We also

349 observed that most m/lEVs derived from erythrocytes and macrophages were Annexin V positive

350 (Fig. 4 N and O). By contrast, many Annexin V negative m/lEVs were identified among platelet-

351 and T and B cell-derived m/lEVs (Fig. 4 P and Q). Especially about erythrocyte-derived m/lEVs

352 other studies have shown high percentages of phosphatidylserine-positive(:Annexin V positive)

353 m/lEVs after red blood cell storage under blood bank conditions that these results are consistent

354 (Gao et al. 2013)(Xiong et al. 2011).

355 In general, it is known that microparicle in blood are known to be exposed to PS on the

356 surface, which is verified by being positive by Annexin5 staining. We found that the degree of

357 exposure of phosphatidylserine to the membrane surface was vary depending on the cell derived

358 from annexin V staining. Thus, the characteristics of m/lEVs can be determined in detail by

359 using AnnexinV and antigenicity. These results suggested that the degree of exposing PS are

360 cell-type specific and that release mechanisms may differ among cell types.

361 **Characterization of urinary EVs by flow cytometry and enzyme activity assay.**

362 In urine, we first removed aggregated m/lEVs and residual THP polymers using labelled

363 normal mouse IgG (Supplementary Fig.S2C). By removing the THP polymer by DTT treatment,

364 many immunological non-specific reactions in flow cytometry observation were eliminated, and

365 the remaining non-specific reactions were completely excluded from the observed image by

366 mouse IgG-positive gating-out (Supplementary Fig.S2F). To characterize urinary m/lEVs, we

367 used surface antigens detected by shotgun proteomic analysis including CD10 (neprilysin),

368 CD13 (alanine aminopeptidase), CD26 (DPP4) and CD227 (MUC1) (Fig. 5A–F). Many m/lEVs

369 in the observation area were triple-positive for CD10, CD13 and CD26, but negative for Annexin

370 V (Fig. 5B–D, Supplementary Fig. S6). Furthermore, MUC1-positive EVs were both Annexin V

371   positive and negative in roughly equivalent frequencies (Fig. 5B, E and F). These results

372   suggested that m/lEVs containing peptidases were released by outward budding directly from the

373   cilial membrane of renal proximal tubule epithelial cells. The results of integrating these

374   characterizations and the distribution of EV classifications among ten healthy subjects are shown

375   (Fig. 5G–I). These data indicated no major differences in the ratio among these populations,

376   suggesting that our methodology was reliable for m/lEV analysis.

377   We next verified the CD26 peptidase enzyme activities of m/lEVs in plasma and urine

378   from six individuals. We prepared three fractions: (i) "whole," in which debris were removed

379   after low speed centrifugation, (ii) "m/lEVs" and (iii) "free (supernatant)" both of which were

380   obtained via high speed centrifugation (18,900 $\times g$ for 30 min) (Fig. 5J). We found that more than

381   20% of DPP4 activity in whole urine was contributed by the EV fraction (Fig. 5K and

382   Supplementary Fig. S7). By contrast, there was no peptidase activity associated with plasma

383   m/lEVs (Fig. 5L). These results suggested that functional CD26 peptidase activity is present in

384   m/lEVs in urine, which may be useful for pathological analysis.

385

386   **Discussion**

387   In this study, we analyzed m/lEVs using various analytic techniques and found the

388   following four major results. First, it was possible to characterize m/lEVs using multiple surface

389   markers. Second, m/lEVs bear functional enzymes with demonstrable enzyme activity on the

390   vesicle surface. Trird, there are probability of differences in asymmetry of membrane lipids by

391   derived cells. Finally, there was little variation m/lEVs in the plasma and urine of healthy

392   individuals, indicating that our method is useful for identifying cell-derived m/lEVs in these

393   body fluids.

394   We isolated m/lEVs from plasma and urine that were primarily 200–800 nm in diameter

395   as shown by transmission electron microscopy. A large proportion of proteins detected in

396   m/lEVs using shotgun proteomic analysis were categorized as plasma membrane proteins.

397   Isolation of m/lEVs by centrifugation is a classical technique, but in the present study we further

398   separated and classified the m/lEVs according to their cell types of origin by flow cytometry.

399   The results indicated the validity of the differential centrifugation method (Biro et al. 2003;

400   Piccin et al. 2015a).

401   Pang et al. (Pang et al. 2018) reported that integrin outside-in signaling is an important

402   mechanism for microvesicle formation, in which the procoagulant phospholipid

403   phosphatidylserine (PS) is efficiently externalized to release PS-exposed microvesicles (MVs).

404   These platelet-derived Annexin V positive MVs were induced by application of a pulling force

405   via an integrin ligand such as shear stress. This exposure of PS allows binding of important

406   coagulation factors, enhancing the catalytic efficiencies of coagulation enzymes. We observed

407   that 50% of m/lEVs derived from leukocytes and platelets were Annexin V positive, suggesting

408   that release PS-positive m/lEVs during activation, inflammation, and injury. It would be

409   interesting to further investigate whether the ratio of Annexin V positive m/lEVs from platelets

410   or leukocytes was an important diagnostic factor for inflammatory disease or tissue injury.

411   In urinary m/lEVs, we identified aminopeptidases such as CD10, CD13 and CD26

412   which are localized in proximal renal tubular epithelial cells. The functions of these proteins

413   relating to exocytosis were categorized by gene enrichment analysis. The cilium in the kidney is

414   the site at which a variety of membrane receptors, enzymes and signal transduction molecules

415   critical to many cellular processes function. In recent years, ciliary ectosomes – bioactive

416   vesicles released from the surface of the cilium – have attracted attention (Nager et al. 2017;

417   Phua et al. 2017; Wood & Rosenbaum 2015). We also identified ciliary ectosome formation

418   ESCRT complexes proteins (CHAMP; Supplementary Table S3 and 4) in proteomic analyses,

419   suggesting that the possibility that these proteins were biomarkers of kidney disease. Because

420   triple peptidase positive m/lEVs were negative for Annexin V, the mechanism of budding from

421   cells may not be dependent on scramblase. (Wood & Rosenbaum 2015)

422   Platelet-derived m/lEVs are the most abundant population of extracellular vesicles in

423   blood, and their presence (Piccin et al. 2007) and connection with tumor formation were reported

424   in a recent study (Zmigrodzka et al. 2016). In our study, platelet-derived EVs were observed in

425   healthy subjects and had the highest abundance of Annexin V-positive EVs. In plasma,

426   leukocyte-derived EVs were defined as CD11b/CD66b- or CD15-positive (Sarlon-Bartoli et al.

427   2013). We characterized macrophage/monocyte/granulocyte- and T/B cell-derived EVs based on

428   two specific CD antigens, and we confirmed that EVs derived from these cells were very rare.

429   Importantly, there was little variation in the cellular origins of m/lEVs in samples from ten

430   healthy individuals, indicating that this method was useful for identifying cell-derived m/lEVs.

431   We plan to examine m/lEVs differences in patients with these diseases in the near future.

432   Erythrocyte-derived EVs were also characterized by their expression of CD235a and glycophorin

433   A by flow cytometry (Ferru et al. 2014; Zecher et al. 2014).

434   We also characterized m/lEVs in urine. In kidneys and particularly in the renal tubule,

435   CD10, CD13, CD26 can be detected in high abundance by immunohistochemical staining

436   (website: The Human Protein Atlas). CD10/CD13-double positive labeling can be used for

437   isolation and characterization of primary proximal tubular epithelial cells from human kidney

438   (Van der Hauwaert et al. 2013). DPP4 (CD26) is a potential biomarker in urine for diabetic

439   kidney disease and the presence of urinary m/lEV-bound DPP4 has been demonstrated (Sun et

440   al. 2012). The presence of peptidases on the m/lEV surface, and their major contribution to

441   peptidase activity in whole urine (Sun et al. 2012), may suggest a functional contribution to

442 reabsorption in the proximal tubules. These observations suggested that the ratio of DPP activity

443 between m/lEVs and total urine can be an important factor in the diagnosis of kidney disease.

444 MUC1 can also be detected in kidney and urinary bladder by immunohistochemical

445 staining (website: The Human Protein Atlas). Significant increases of MUC1 expression in

446 cancerous tissue and in the intermediate zone compared with normal renal tissue distant from the

447 tumor was observed (Borzym-Kluczyk et al. 2015). In any case, MUC1-positive EVs are thought

448 to be more likely to be derived from the tubular epithelium or the urothelium.

449

Conclusions

451 Use of EVs as diagnostic reagents with superior disease and organ specificity for liquid

452 biopsy samples is a possibility. This protocol will allow further study and in depth

453 characterization of EV profiles in large patient groups for clinical applications. We are going to

454 attempt to identify novel biomarkers by comparing healthy subjects and patients with various

455 diseases.

456

457 **ACKNOWLEDGEMENTS**

458 We thank lab members for reagents, discussions, and critical reading of the manuscript. We are

459 grateful to LSI Medience Corporation for generous support during this study. This work was

460 supported by a Grant-in-Aid for Scientific Research from the Japan Society for the Promotion of

461 Science (JSPS; grant numbers #25253041, #17H01550 and 15H04764) and research funding

462 from LSI Medience Corporation. We thank Edanz Group (www.edanzediting.com/ac) for editing

463 a draft of this manuscript.

464

465 **Author Contributions**

466 K.I. and T.U. designed the research and wrote the manuscript. S.U., K.G., S.M. and M.A carried

467 out the experiments, obtained reagents and materials, and conducted data analysis. D.S. and N.A.

468 contributed to network analysis. D.K, K.K. and T.U. contributed to flavonoid identification. All

469 authors read and approved the final manuscript.

470

471 **Competing Interests**

472 The authors have read the journal's policy and would like to declare the following competing

473 interests: K.I. is a full-time employee of LSI Medience Corporation. K.K. is a full-time employee

474 of LSI Medience Corporation. K.I. is also seconded to Kyushu Pro Search Limited Liability

475 Partnership from LSI Medience Corporation. K.K. also serves as Kyushu Pro Search Limited

476 Liability Partnership and LSI Medience Corporation and is the representative officer of Kyushu

477 Pro Search Limited Liability Partnership.

478

479

480

481 **Reference**

482 Biro E, Sturk-Maquelin KN, Vogel GM, Meuleman DG, Smit MJ, Hack CE, Sturk A, and Nieuwland R.
483   2003. Human cell-derived microparticles promote thrombus formation in vivo in a tissue factor-
484   dependent manner. *J Thromb Haemost* 1:2561-2568.

485 Borzym-Kluczyk M, Radziejewska I, and Cechowska-Pasko M. 2015. Increased expression of MUC1 and
486   sialyl Lewis antigens in different areas of clear renal cell carcinoma. *Clin Exp Nephrol* 19:732-737.
487   10.1007/s10157-014-1013-y

488 Boukouris S, and Mathivanan S. 2015. Exosomes in bodily fluids are a highly stable resource of disease
489   biomarkers. *Proteomics Clin Appl* 9:358-367. 10.1002/prca.201400114

490 Chen IH, Xue L, Hsu CC, Paez JS, Pan L, Andaluz H, Wendt MK, Iliuk AB, Zhu JK, and Tao WA. 2017.
491   Phosphoproteins in extracellular vesicles as candidate markers for breast cancer. *Proc Natl Acad*
492   *Sci U S A* 114:3175-3180. 10.1073/pnas.1618088114

493 Clancy JW, Sedgwick A, Rosse C, Muralidharan-Chari V, Raposo G, Method M, Chavrier P, and D'Souza-
494   Schorey C. 2015. Regulated delivery of molecular cargo to invasive tumour-derived microvesicles.
495   *Nat Commun* 6:6919. 10.1038/ncomms7919

496 D'Souza-Schorey C, and Clancy JW. 2012. Tumor-derived microvesicles: shedding light on novel
497   microenvironment modulators and prospective cancer biomarkers. *Genes Dev* 26:1287-1299.
498   10.1101/gad.192351.112

499 El Andaloussi S, Lakhal S, Mager I, and Wood MJ. 2013. Exosomes for targeted siRNA delivery across
500   biological barriers. *Adv Drug Deliv Rev* 65:391-397. 10.1016/j.addr.2012.08.008

501 Fernandez-Llama P, Khositseth S, Gonzales PA, Star RA, Pisitkun T, and Knepper MA. 2010. Tamm-
502   Horsfall protein and urinary exosome isolation. *Kidney Int* 77:736-742. 10.1038/ki.2009.550

503 Ferru E, Pantaleo A, Carta F, Mannu F, Khadjavi A, Gallo V, Ronzoni L, Graziadei G, Cappellini MD, and
504   Turrini F. 2014. Thalassemic erythrocytes release microparticles loaded with hemichromes by
505   redox activation of p72Syk kinase. *Haematologica* 99:570-578. 10.3324/haematol.2013.084533

506 Gao Y, Lv L, Liu S, Ma G, and Su Y. 2013. Elevated levels of thrombin‐generating microparticles in
507   stored red blood cells. *Vox sanguinis* 105:11-17.

508 Iraci N, Leonardi T, Gessler F, Vega B, and Pluchino S. 2016. Focus on Extracellular Vesicles:
509   Physiological Role and Signalling Properties of Extracellular Membrane Vesicles. *Int J Mol Sci*
510   17:171. 10.3390/ijms17020171

511 Jayachandran M, Miller VM, Heit JA, and Owen WG. 2012. Methodology for isolation, identification and
512   characterization of microvesicles in peripheral blood. *J Immunol Methods* 375:207-214.
513   10.1016/j.jim.2011.10.012

514   Kawaguchi M, Okabe T, Terai T, Hanaoka K, Kojima H, Minegishi I, and Nagano T. 2010. A time-resolved
515   fluorescence probe for dipeptidyl peptidase 4 and its application in inhibitor screening. *Chemistry*
516   16:13479-13486. 10.1002/chem.201001077
517   Mateescu B, Kowal EJ, van Balkom BW, Bartel S, Bhattacharyya SN, Buzas EI, Buck AH, de Candia P,
518   Chow FW, Das S, Driedonks TA, Fernandez-Messina L, Haderk F, Hill AF, Jones JC, Van Keuren-
519   Jensen KR, Lai CP, Lasser C, Liegro ID, Lunavat TR, Lorenowicz MJ, Maas SL, Mager I,
520   Mittelbrunn M, Momma S, Mukherjee K, Nawaz M, Pegtel DM, Pfaffl MW, Schiffelers RM,
521   Tahara H, Thery C, Tosar JP, Wauben MH, Witwer KW, and Nolte-'t Hoen EN. 2017. Obstacles
522   and opportunities in the functional analysis of extracellular vesicle RNA - an ISEV position paper.
523   *J Extracell Vesicles* 6:1286095. 10.1080/20013078.2017.1286095
524   Mathivanan S, Ji H, and Simpson RJ. 2010. Exosomes: extracellular organelles important in intercellular
525   communication. *J Proteomics* 73:1907-1920. 10.1016/j.jprot.2010.06.006
526   Nager AR, Goldstein JS, Herranz-Perez V, Portran D, Ye F, Garcia-Verdugo JM, and Nachury MV. 2017.
527   An Actin Network Dispatches Ciliary GPCRs into Extracellular Vesicles to Modulate Signaling.
528   *Cell* 168:252-263 e214. 10.1016/j.cell.2016.11.036
529   Ohno S, Ishikawa A, and Kuroda M. 2013. Roles of exosomes and microvesicles in disease pathogenesis.
530   *Adv Drug Deliv Rev* 65:398-401. 10.1016/j.addr.2012.07.019
531   Pang A, Cui Y, Chen Y, Cheng N, Delaney MK, Gu M, Stojanovic-Terpo A, Zhu C, and Du X. 2018.
532   Shear-induced integrin signaling in platelet phosphatidylserine exposure, microvesicle release, and
533   coagulation. *Blood* 132:533-543. 10.1182/blood-2017-05-785253
534   Phua SC, Chiba S, Suzuki M, Su E, Roberson EC, Pusapati GV, Setou M, Rohatgi R, Reiter JF, Ikegami
535   K, and Inoue T. 2017. Dynamic Remodeling of Membrane Composition Drives Cell Cycle through
536   Primary Cilia Excision. *Cell* 168:264-279 e215. 10.1016/j.cell.2016.12.032
537   Piccin A. 2014. Endothelial Microparticles and Endothelial Damage:'The Tip and the Iceberg'. *Acta*
538   *haematologica* 132:199-199.
539   Piccin A, Murphy C, Eakins E, Kunde J, Corvetta D, Di Pierro A, Negri G, Guido M, Sainati L, Mc Mahon
540   C, Smith OP, and Murphy W. 2015a. Circulating microparticles, protein C, free protein S and
541   endothelial vascular markers in children with sickle cell anaemia. *J Extracell Vesicles* 4:28414.
542   10.3402/jev.v4.28414
543   Piccin A, Murphy WG, and Smith OP. 2007. Circulating microparticles: pathophysiology and clinical
544   implications. *Blood Rev* 21:157-171. 10.1016/j.blre.2006.09.001
545   Piccin A, Sartori MT, Bisogno G, Van Schilfgaarde M, Saggiorato G, Pierro AM, Corvetta D, Marcheselli
546   L, Andrea M, and Gastl G. 2017a. New insights into sinusoidal obstruction syndrome. *Internal*
547   *medicine journal* 47:1173-1183.

548   Piccin A, Steurer M, Feistritzer C, Murphy C, Eakins E, Van Schilfgaarde M, Corvetta D, Di Pierro AM,
549   Pusceddu I, and Marcheselli L. 2017b. Observational retrospective study of vascular modulator
550   changes during treatment in essential thrombocythemia. *Translational Research* 184:21-34.
551   Piccin A, Van Schilfgaarde M, and Smith O. 2015b. The importance of studying red blood cells
552   microparticles. *Blood Transfusion* 13:172.
553   Raposo G, and Stoorvogel W. 2013. Extracellular vesicles: exosomes, microvesicles, and friends. *J Cell
554   Biol* 200:373-383. 10.1083/jcb.201211138
555   Robbins PD, and Morelli AE. 2014. Regulation of immune responses by extracellular vesicles. *Nat Rev
556   Immunol* 14:195-208. 10.1038/nri3622
557   Sarlon-Bartoli G, Bennis Y, Lacroix R, Piercecchi-Marti MD, Bartoli MA, Arnaud L, Mancini J, Boudes
558   A, Sarlon E, Thevenin B, Leroyer AS, Squarcioni C, Magnan PE, Dignat-George F, and Sabatier
559   F. 2013. Plasmatic level of leukocyte-derived microparticles is associated with unstable plaque in
560   asymptomatic patients with high-grade carotid stenosis. *J Am Coll Cardiol* 62:1436-1441.
561   10.1016/j.jacc.2013.03.078
562   Smalley DM, Sheman NE, Nelson K, and Theodorescu D. 2008. Isolation and identification of potential
563   urinary microparticle biomarkers of bladder cancer. *J Proteome Res* 7:2088-2096.
564   10.1021/pr700775x
565   Sun AL, Deng JT, Guan GJ, Chen SH, Liu YT, Cheng J, Li ZW, Zhuang XH, Sun FD, and Deng HP. 2012.
566   Dipeptidyl peptidase-IV is a potential molecular biomarker in diabetic kidney disease. *Diab Vasc
567   Dis Res* 9:301-308. 10.1177/1479164111434318
568   Thery C, Witwer KW, Aikawa E, Alcaraz MJ, Anderson JD, Andriantsitohaina R, Antoniou A, Arab T,
569   Archer F, Atkin-Smith GK, Ayre DC, Bach JM, Bachurski D, Baharvand H, Balaj L, Baldacchino
570   S, Bauer NN, Baxter AA, Bebawy M, Beckham C, Bedina Zavec A, Benmoussa A, Berardi AC,
571   Bergese P, Bielska E, Blenkiron C, Bobis-Wozowicz S, Boilard E, Boireau W, Bongiovanni A,
572   Borras FE, Bosch S, Boulanger CM, Breakefield X, Breglio AM, Brennan MA, Brigstock DR,
573   Brisson A, Broekman ML, Bromberg JF, Bryl-Gorecka P, Buch S, Buck AH, Burger D, Busatto S,
574   Buschmann D, Bussolati B, Buzas EI, Byrd JB, Camussi G, Carter DR, Caruso S, Chamley LW,
575   Chang YT, Chen C, Chen S, Cheng L, Chin AR, Clayton A, Clerici SP, Cocks A, Cocucci E, Coffey
576   RJ, Cordeiro-da-Silva A, Couch Y, Coumans FA, Coyle B, Crescitelli R, Criado MF, D'Souza-
577   Schorey C, Das S, Datta Chaudhuri A, de Candia P, De Santana EF, De Wever O, Del Portillo HA,
578   Demaret T, Deville S, Devitt A, Dhondt B, Di Vizio D, Dieterich LC, Dolo V, Dominguez Rubio
579   AP, Dominici M, Dourado MR, Driedonks TA, Duarte FV, Duncan HM, Eichenberger RM,
580   Ekstrom K, El Andaloussi S, Elie-Caille C, Erdbrugger U, Falcon-Perez JM, Fatima F, Fish JE,
581   Flores-Bellver M, Forsonits A, Frelet-Barrand A, Fricke F, Fuhrmann G, Gabrielsson S, Gamez-
582   Valero A, Gardiner C, Gartner K, Gaudin R, Gho YS, Giebel B, Gilbert C, Gimona M, Giusti I,
583   Goberdhan DC, Gorgens A, Gorski SM, Greening DW, Gross JC, Gualerzi A, Gupta GN,

584   Gustafson D, Handberg A, Haraszti RA, Harrison P, Hegyesi H, Hendrix A, Hill AF, Hochberg
585   FH, Hoffmann KF, Holder B, Holthofer H, Hosseinkhani B, Hu G, Huang Y, Huber V, Hunt S,
586   Ibrahim AG, Ikezu T, Inal JM, Isin M, Ivanova A, Jackson HK, Jacobsen S, Jay SM, Jayachandran
587   M, Jenster G, Jiang L, Johnson SM, Jones JC, Jong A, Jovanovic-Talisman T, Jung S, Kalluri R,
588   Kano SI, Kaur S, Kawamura Y, Keller ET, Khamari D, Khomyakova E, Khvorova A, Kierulf P,
589   Kim KP, Kislinger T, Klingeborn M, Klinke DJ, 2nd, Kornek M, Kosanovic MM, Kovacs AF,
590   Kramer-Albers EM, Krasemann S, Krause M, Kurochkin IV, Kusuma GD, Kuypers S, Laitinen S,
591   Langevin SM, Languino LR, Lannigan J, Lasser C, Laurent LC, Lavieu G, Lazaro-Ibanez E, Le
592   Lay S, Lee MS, Lee YXF, Lemos DS, Lenassi M, Leszczynska A, Li IT, Liao K, Libregts SF,
593   Ligeti E, Lim R, Lim SK, Line A, Linnemannstons K, Llorente A, Lombard CA, Lorenowicz MJ,
594   Lorincz AM, Lotvall J, Lovett J, Lowry MC, Loyer X, Lu Q, Lukomska B, Lunavat TR, Maas SL,
595   Malhi H, Marcilla A, Mariani J, Mariscal J, Martens-Uzunova ES, Martin-Jaular L, Martinez MC,
596   Martins VR, Mathieu M, Mathivanan S, Maugeri M, McGinnis LK, McVey MJ, Meckes DG, Jr.,
597   Meehan KL, Mertens I, Minciacchi VR, Moller A, Moller Jorgensen M, Morales-Kastresana A,
598   Morhayim J, Mullier F, Muraca M, Musante L, Mussack V, Muth DC, Myburgh KH, Najrana T,
599   Nawaz M, Nazarenko I, Nejsum P, Neri C, Neri T, Nieuwland R, Nimrichter L, Nolan JP, Nolte-'t
600   Hoen EN, Noren Hooten N, O'Driscoll L, O'Grady T, O'Loghlen A, Ochiya T, Olivier M, Ortiz A,
601   Ortiz LA, Osteikoetxea X, Ostergaard O, Ostrowski M, Park J, Pegtel DM, Peinado H, Perut F,
602   Pfaffl MW, Phinney DG, Pieters BC, Pink RC, Pisetsky DS, Pogge von Strandmann E,
603   Polakovicova I, Poon IK, Powell BH, Prada I, Pulliam L, Quesenberry P, Radeghieri A, Raffai RL,
604   Raimondo S, Rak J, Ramirez MI, Raposo G, Rayyan MS, Regev-Rudzki N, Ricklefs FL, Robbins
605   PD, Roberts DD, Rodrigues SC, Rohde E, Rome S, Rouschop KM, Rughetti A, Russell AE, Saa P,
606   Sahoo S, Salas-Huenuleo E, Sanchez C, Saugstad JA, Saul MJ, Schiffelers RM, Schneider R,
607   Schoyen TH, Scott A, Shahaj E, Sharma S, Shatnyeva O, Shekari F, Shelke GV, Shetty AK, Shiba
608   K, Siljander PR, Silva AM, Skowronek A, Snyder OL, 2nd, Soares RP, Sodar BW, Soekmadji C,
609   Sotillo J, Stahl PD, Stoorvogel W, Stott SL, Strasser EF, Swift S, Tahara H, Tewari M, Timms K,
610   Tiwari S, Tixeira R, Tkach M, Toh WS, Tomasini R, Torrecilhas AC, Tosar JP, Toxavidis V,
611   Urbanelli L, Vader P, van Balkom BW, van der Grein SG, Van Deun J, van Herwijnen MJ, Van
612   Keuren-Jensen K, van Niel G, van Royen ME, van Wijnen AJ, Vasconcelos MH, Vechetti IJ, Jr.,
613   Veit TD, Vella LJ, Velot E, Verweij FJ, Vestad B, Vinas JL, Visnovitz T, Vukman KV, Wahlgren
614   J, Watson DC, Wauben MH, Weaver A, Webber JP, Weber V, Wehman AM, Weiss DJ, Welsh JA,
615   Wendt S, Wheelock AM, Wiener Z, Witte L, Wolfram J, Xagorari A, Xander P, Xu J, Yan X,
616   Yanez-Mo M, Yin H, Yuana Y, Zappulli V, Zarubova J, Zekas V, Zhang JY, Zhao Z, Zheng L,
617   Zheutlin AR, Zickler AM, Zimmermann P, Zivkovic AM, Zocco D, and Zuba-Surma EK. 2018.
618   Minimal information for studies of extracellular vesicles 2018 (MISEV2018): a position statement

619 of the International Society for Extracellular Vesicles and update of the MISEV2014 guidelines. *J*
620 *Extracell Vesicles* 7:1535750. 10.1080/20013078.2018.1535750

621 Van der Hauwaert C, Savary G, Gnemmi V, Glowacki F, Pottier N, Bouillez A, Maboudou P, Zini L, Leroy
622 X, Cauffiez C, Perrais M, and Aubert S. 2013. Isolation and characterization of a primary proximal
623 tubular epithelial cell model from human kidney by CD10/CD13 double labeling. *PLoS One*
624 8:e66750. 10.1371/journal.pone.0066750

625 Wood CR, and Rosenbaum JL. 2015. Ciliary ectosomes: transmissions from the cell's antenna. *Trends Cell*
626 *Biol* 25:276-285. 10.1016/j.tcb.2014.12.008

627 Xiong Z, Cavaretta J, Qu L, Stolz DB, Triulzi D, and Lee JS. 2011. Red blood cell microparticles show
628 altered inflammatory chemokine binding and release ligand upon interaction with platelets.
629 *Transfusion* 51:610-621.

630 Yoshioka Y, Kosaka N, Konishi Y, Ohta H, Okamoto H, Sonoda H, Nonaka R, Yamamoto H, Ishii H, Mori
631 M, Furuta K, Nakajima T, Hayashi H, Sugisaki H, Higashimoto H, Kato T, Takeshita F, and Ochiya
632 T. 2014. Ultra-sensitive liquid biopsy of circulating extracellular vesicles using ExoScreen. *Nat*
633 *Commun* 5:3591. 10.1038/ncomms4591

634 Zecher D, Cumpelik A, and Schifferli JA. 2014. Erythrocyte-derived microvesicles amplify systemic
635 inflammation by thrombin-dependent activation of complement. *Arterioscler Thromb Vasc Biol*
636 34:313-320. 10.1161/ATVBAHA.113.302378

637 Zmigrodzka M, Guzera M, Miskiewicz A, Jagielski D, and Winnicka A. 2016. The biology of extracellular
638 vesicles with focus on platelet microparticles and their role in cancer development and progression.
639 *Tumour Biol* 37:14391-14401. 10.1007/s13277-016-5358-6

640

641

Twenty most abundant proteins identified in plasma m/lEVs

1   **Table 1.   Twenty most abundant proteins identified in plasma m/lEVs**

Protein name	Uniprot AC	Score	Sequence coverage
Ficolin-3	O75636	8772	68
Hemoglobin subunit alpha	P69905	1735	70
Actin, cytoplasmic 1	P60709	927	69
Hemoglobin subunit beta	P68871	602	79
Actin, gamma-enteric smooth muscle	P63267	500	32
Talin-1	Q9Y490	368	50
Filamin-A	P21333	353	40
Spectrin alpha chain, erythrocytic 1	P02549	321	42
Myosin-9	P35579	317	38
Mannan-binding lectin serine protease 1	P48740	308	35
Band 3 anion transport protein	P02730	277	38
Beta-actin-like protein 2	Q562R1	252	24
Hemoglobin subunit delta	P02042	215	64
Spectrin beta chain, erythrocytic	P11277	183	28
Complement C1q subcomponent subunit C	P02747	170	24
Ankyrin-1	P16157	164	28
CD5 antigen-like	O43866	164	52
Integrin alpha-IIb (CD41)	P08514	129	25
Complement C1q subcomponent subunit B	P02746	122	41
Deaminated glutathione amidase	Q86X76	118	6

2   Proteins in bold text indicate antigens identified using flow cytometry. This table excluded

3   immunoglobulin-related proteins and albumin.

Twenty most abundant proteins identified in urinary m/lEVs

1   **Table 2.   Twenty most abundant proteins identified in urinary m/lEVs**

Protein name	Uniprot AC	Score	Sequence coverage
Actin, cytoplasmic 1	P60709	1618	67
Neprilysin	P08473	1194	50
Uromodulin	P07911	821	44
Solute carrier family 12 member 1	Q13621	720	32
Alpha-enolase	P06733	708	79
Moesin	P26038	548	73
Ezrin	P15311	544	56
Aminopeptidase N	P15144	486	43
Actin, gamma-enteric smooth muscle	P63267	476	28
Pyruvate kinase PKM	P14618	447	64
Voltage-dependent anion-selective channel protein 1	P21796	446	74
Radixin	P35241	364	56
Tyrosine-protein phosphatase non-receptor type 13	Q12923	363	38
Triosephosphate isomerase	P60174	325	80
Multidrug resistance protein 1	P08183	324	38
Guanine nucleotide-binding protein G(I)/G(S)/G(T) subunit beta-2	P62879	316	50
Guanine nucleotide-binding protein G(I)/G(S)/G(T) subunit beta-1	P62873	306	53
V-type proton ATPase catalytic subunit A	P38606	298	57
Superoxide dismutase [Cu-Zn]	P00441	285	91
Epidermal growth factor receptor kinase substrate 8-like protein 2	Q9H6S3	277	43

2   Proteins in bold text indicate antigens identified using flow cytometry

Figure 1

Isolation of m/lEVs from plasma and urine using differential centrifugation

(A and B) Workflow of plasma (A) and urine (B) m/lEV isolation and sample preparation for flow cytometry analysis. (C–H) Isolated m/lEVs from plasma (C–E) and urine (F–H) were visualized by transmission electron microscopy. Arrow indicates representative m/lEVs (C and F). Microscopy was used to identify EV-like particles based on the size (100–400 nm) and shape (round) of the vesicles. The scale bar is shown.
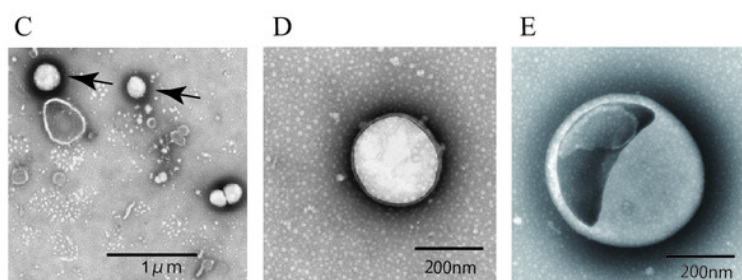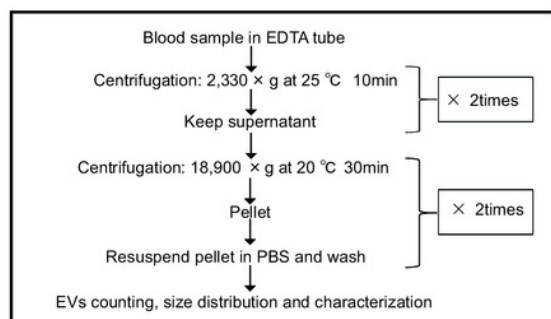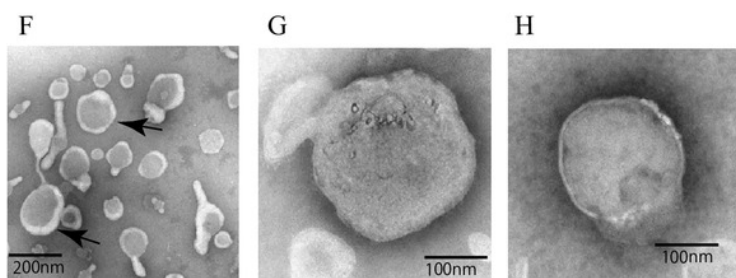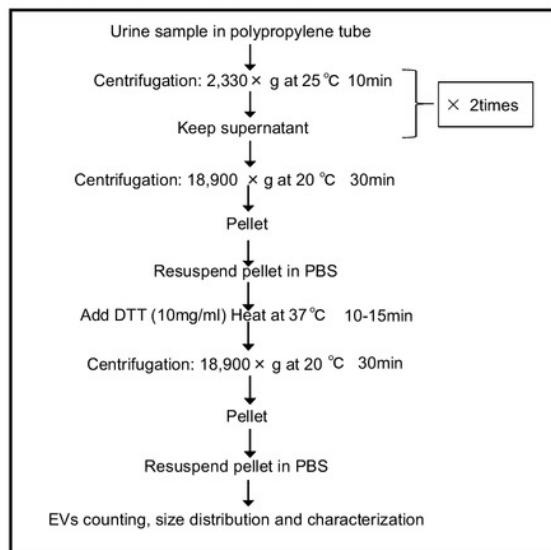
Figure 2

Flow cytometric analysis of plasma and urine m/lEVs

(A and B) Analysis of plasma m/lEVs by flow cytometry. Forward and side scatter (SSC) were measured for plasma m/lEVs (A). The SSC distribution of plasma m/lEVs is shown as a histogram (indigo blue) compared with standard polystyrene beads (black histogram) (B). (C and D) Analysis of urine m/lEVs by flow cytometry. Forward and side scatter (SSC) were measured for urine m/lEVs (C). The SSC distribution of urinary m/lEVs is shown as a histogram (orange) compared with standard polystyrene beads (black histogram) (D).

Plasma m/lEVs

Urine m/lEVs
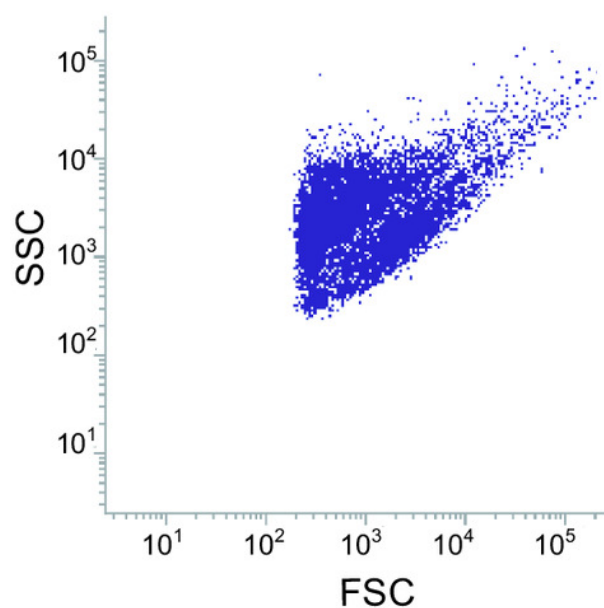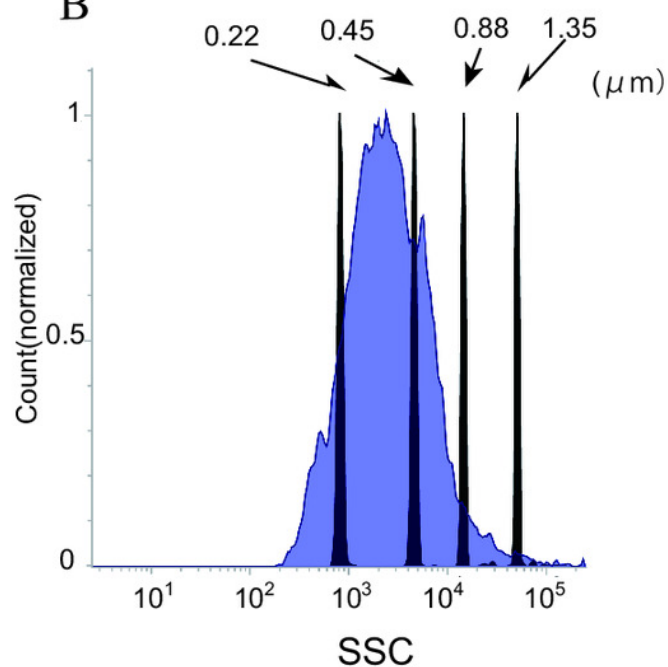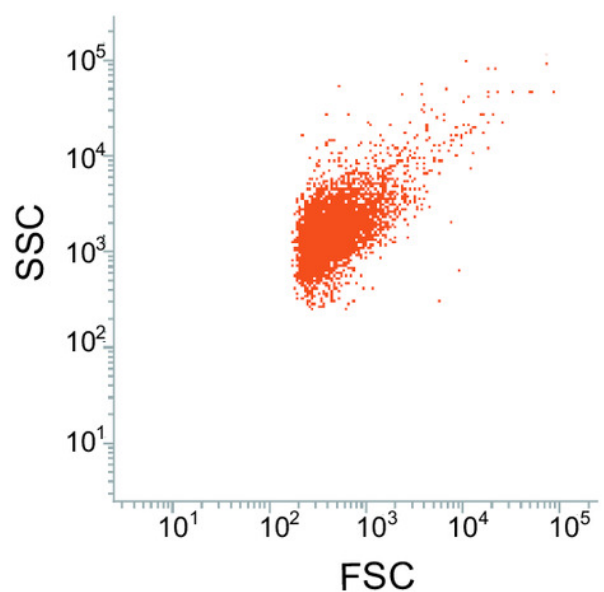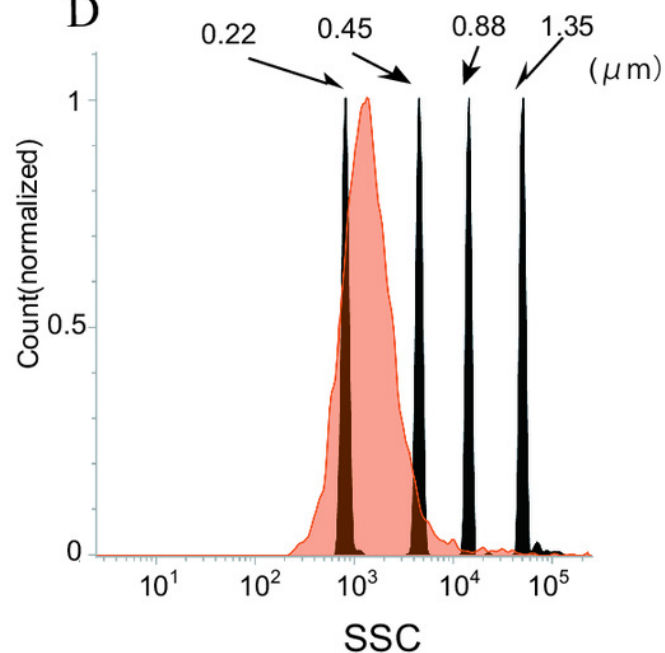
Figure 3

Shotgun proteomic analysis of plasma and urine m/lEVs

A. Protein extracts of m/lEVs isolated from plasma and urine were analyzed by LC-MS/MS. A total of 593 and 1793 proteins from plasma and urine, respectively, were detected. Detailed lists of proteins are shown in S1 Table and S2 Table. B. GO (gene ontology) cellular components are shown for m/lEVs isolated from plasma and urine using the DAVID program. Among the detected proteins, the gene list used for DAVID analysis included 588 proteins (plasma) and 1786 proteins (urine). The vertical axis shows the percentage of proteins from the full gene list categorized into each GO term. For example, for extracellular exosomes (plasma), the categorized count was 301 of 588 proteins. (C and D) Top 20 clusters from the Metascape pathway (http://metascape.org/) enrichment analysis for m/lEVs in plasma (C) and urine (D). Lengths of bars represent log10 (P values) based on the best-scoring term within each cluster. Among all detected proteins, 535 (plasma) and 1767 (urine) genes were recognized as unique for enrichment analysis. For each gene list, pathway and process enrichment analysis was carried out using the following ontology sources: KEGG Pathway, GO Biological Processes, Reactome Gene Sets, Canonical Pathways and CORUM.

A

Plasma   Urine

375   218   1575

B   Cellular component

D   Urine m/IEVs enrichment analysis
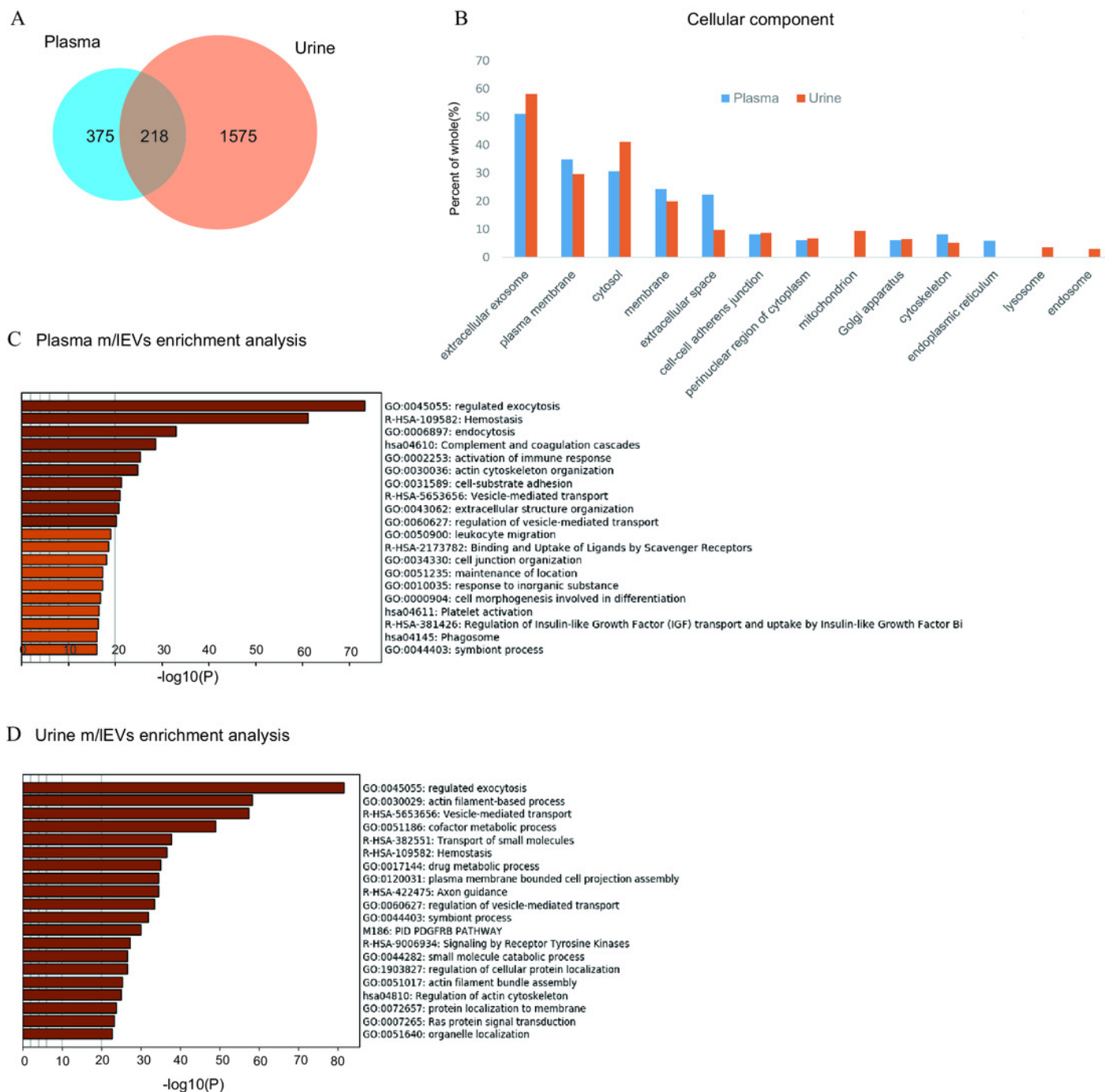
Figure 4

Characterization of plasma m/lEVs by flow cytometry

A. Two specific surface antigens were used to characterize the m/lEVs from each source by flow cytometry. m/lEVs were characterized by comparison with five types of blood cells using surface antigens and Annexin V staining. (B–L). Representative dot plots (SSC vs. Annexin V). Each plot was classified by staining for surface antigens and Annexin V (C–L) and an overall plot summarizing the data (B) is shown. M. Quantification of each m/lEV by flow cytometry analysis (n=10 for human healthy plasma, % of total events). (N–Q). Comparison of Annexin V staining for erythrocyte-(N), macrophage-(O), platelet-(P) and T and B cell-(Q) derived m/lEVs from ten healthy plasma samples. Comparisons were performed using the Wilcoxon signed-rank test (* p< 0.05, ** p < 0.01; a value of p < 0.05 was considered to indicate statistical significance).

A Plasma m/IEVs characterized by multi CD antigen

	Annexin5	CD59	CD235a	CD41	CD61	CD15	CD45	CD5	CD105	CD146
		·Protectin ·MIRL	·Glycophorin A	·Integrin αIIb	·Integrin β3	·Lewis x ·SSEA-1	·Leukocyte Common Antigen	·Leu-1	·Endoglin	·Muc 18
Erythrocyte derived	+	+	+				-			
	-	+	+				-			
Platelet derived	+			+	+		-	-		
	-			+	+		-	-		
Macrophage/Monocyte/Granulocyte derived	+		-			+	+			
	-		-			+	+			
T and B cell derived	+		-				+	+		
	-		-				+	+		
Endothelial Cell derived	+								+	+
	-								+	+

B (Annexin 5 vs SSC scatter plot)

C Erythrocyte derived **E** Platelet derived **G** Macrophage/Monocyte Granulocyte derived **I** T and B cell derived **K** Endotherial cell derived

Annexin 5 (+ / -) vs SSC plots: C, D, E, F, G, H, I, J, K, L
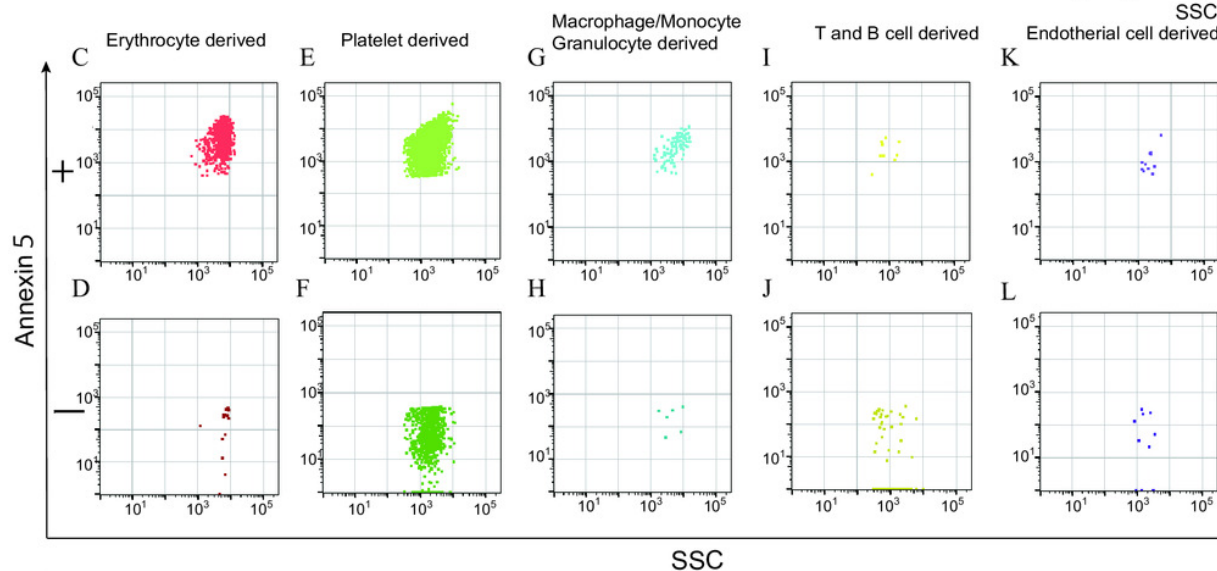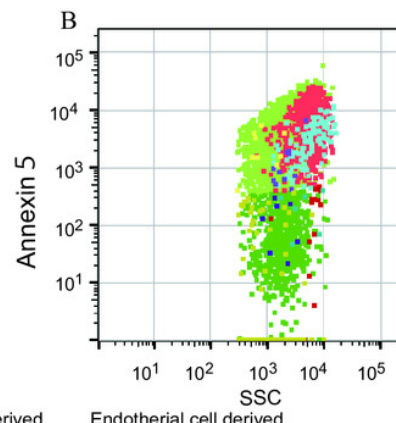
M Characterized m/IEVs ratio in 10 healthy plasma

(N=10)	Annexin5	Average(%)	SD	range (%)
Erythrocyte derived	+	10%	4.2%	2.8-16
	-	0.16%	0.25%	0-0.84
Platelet derived	+	19%	8.2%	4.6-30
	-	16%	10%	2.6-32
Macrophage/Monocyte/Granulocyte derived	+	0.43%	0.49%	0.02-1.3
	-	0.07%	0.10%	0-0.31
T and B cell derived	+	0.19%	0.24%	0.01-0.77
	-	0.50%	0.40%	0.05-1.4
Endothelial Cell derived	+	0.08%	0.05%	0.02-0.2
	-	0.03%	0.03%	0.01-0.09

N Erythrocyte derived ✱✱

O Macrophage/Monocyte Granulocyte derived ✱✱

P Platelet derived

Q T and B cell derived ✱
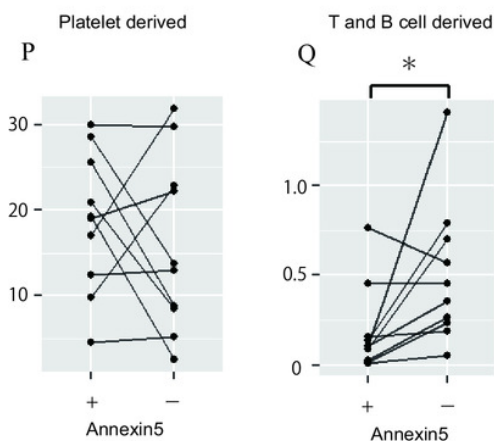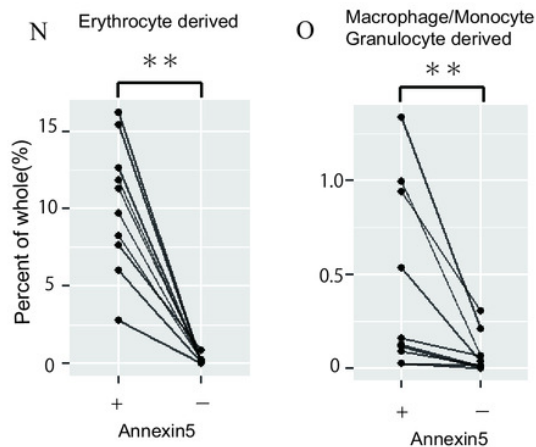
Figure 5

Characterization of urinary m/lEVs by flow cytometry and CD26 enzymatic activity

A. Two kinds of m/lEVs in urine were characterized by using surface antigen and Annexin V staining. (B–F). Representative dot plots in the observation area (SSC vs Annexin V). Each plot was classified according to staining for multiple peptidases [CD10 (neprilysin), CD13 (alanine aminopeptidase) and CD26 (DPP4)] (C and D), and CD277 (MUC-1) (E and F). Events were further classified as Annexin V positive or negative. G. Quantification of m/lEVs by flow cytometry analyses (n=10 for male human healthy urine, % of total events). (H and I). Comparison of Annexin V staining for MUC1-positive (H) and multiple peptidase-positive (I) m/lEVs in the urine of ten healthy male human samples. Comparisons were performed using the Wilcoxon signed-rank test (* P < 0.05, ** P < 0.01; a value of p < 0.05 was considered to indicate statistical significance). J. DPP4 enzymatic activity was assessed for urinary m/lEVs. The workflow for fractionating m/lEVs by centrifugation is shown. (K and L). Quantification of DPP4 activity in urine (K) and plasma (L) fractions (n=6 for human healthy male urine and plasma, % of whole). The percentage of enzyme activity measured for each fraction compared with whole activity is shown.

A Urine m/lEVs characterized by multi CD antigen

	Annexin5	CD10	CD13	CD26	CD227
		· neutral endopeptidase · Neprilysin	· Amino peptidase N	· Dipeptidyl Peptidase-4 (DPPIV)	· Mucin 1 (MUC1)
Multiple peptidase positive	+	+	+	+	-
	-	+	+	+	-
MUC1 positive	+		-		+
	-		-		+

G Characterized m/lEVs ratio in 10 healthy male urine

(N=10)	Annexin5	Average(%)	SD	range (%)
Multiple peptidase (CD10,CD13,CD26) positive	+	10%	9.0%	2.2-28
	-	38%	17%	11-68
MUC1 positive	+	5.2%	3.4%	2.0-12
	-	3.2%	2.6%	0.82-9.4

B

C Multiple peptidase positive

E MUC1 positive

D

F

SSC

Annexin 5

H MUC1 positive

I Multiple peptidase positive

**

Percent of whole(%)

Annexin5
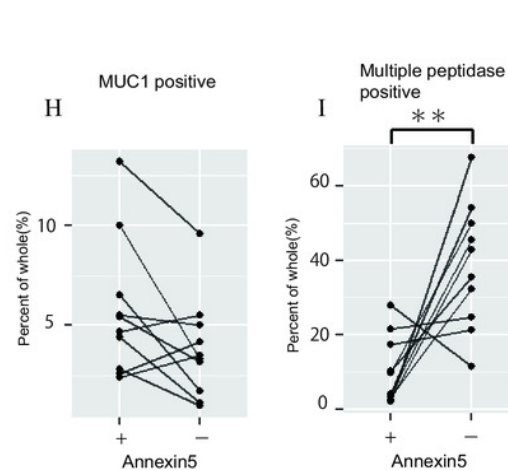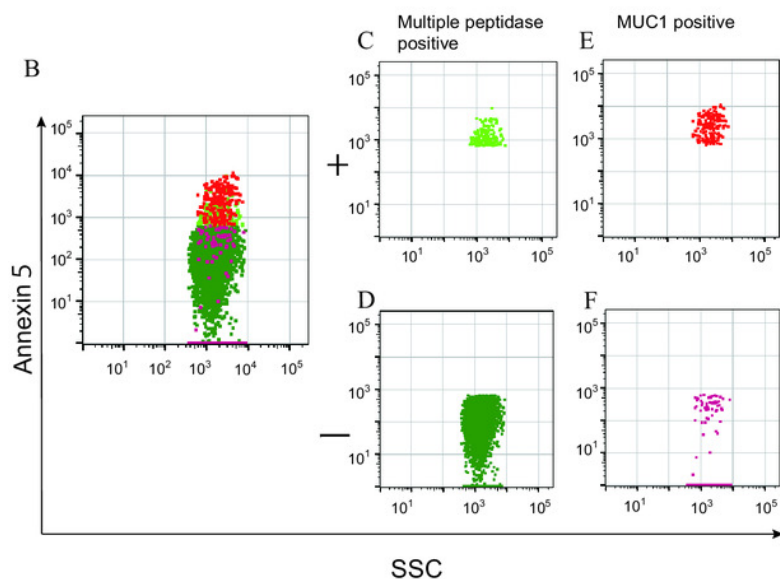
J DPP4(CD26) activity of plasma and urine m/lEVs

Blood sample in EDTA tube or Urine sample in polypropylene tube

Centrifugation: 2,330 × g at 25 ℃ 10min   × 2times

Keep supernatant → Whole activity

Centrifugation: 18,900 × g at 20 ℃ 30min

ppt   supernatant → Supernatant activity

An assay buffer of same volume of whole sample was added → m/lEVs activity

K Urine

L Plasma

Percent of whole(%)

m/lEVs Supernatant Whole